Time domain FWI in Matlab with applications to inversion of simulated VSP data

Ninoska Amundaray and Kris Innanen

ABSTRACT

The optimization function in a full waveform inversion (FWI) iterative scheme is given by the difference between observed and synthetic data. Initial difficulties are traceable to the environment and design of seismic acquisition, which are more complex in land datasets. Recent applications of FWI using vertical seismic profiles (VSP) demonstrate suitable features of these surveys to overcome some inversion challenges. In this report, we analyzed the performance of a standard FWI algorithm with simulated VSP data in Matlab, as a preparatory step to use it with real data. Inverted models converged towards the optimal solution, illustrating how the resolution is controlled by the disposition of sources and receivers in an acquisition survey. Multiscale approaches tested emphasize the usage of frequency bands to reconcile model features with the frequency spectrum of the dataset. Fast convergence of the algorithm is achieved utilizing a reverse time migration (RTM) of the residuals constructed using a crosscorrelation imaging condition, equivalent to the FWI gradient.

INTRODUCTION

Full waveform inversion (FWI) is currently a common method used to compute high-resolution subsurface models by iteratively optimizing an objective function, which in an FWI scheme is given by the difference between the observed and synthetic dataset known as the data residual. One of the key features of this procedure is the utilization of the entire content of the wavefield information to extract the physical parameters of the medium sample using seismic waves. However, in order to solve for those parameters, challenges constantly arise in both data and model spaces.

In the data space, difficulties can be traced to the environment type, survey design and regular downfalls of seismic acquisition, all of which are usually more difficult on land surveys. A predominant and troublesome feature for successful FWI applications using land seismic is a poor signal-to-noise ratio especially for the frequencies in the low end of the spectrum, which are important in FWI to assist model updates to converge to the global minimum.

In connection with land surveys, vertical seismic profiles (VSP) have shown in recent years promising applications of FWI for analysis and monitoring purposes in reservoirs, due to the geometry of the experiment. Since the receivers are secured to the walls of a wellbore, they are often protected against most of the surface-related noise sources providing higher signal-to-noise ratio (Cova et al., 2018).

Applications in conventional (Podgornova et al., 2014) and unconventional reservoirs (Pan et al., 2018) and CO_2 sequestration projects (Egorov et al., 2017) provide incentive for further examination of VSP for FWI applications. Our primary objective is inverting a real VSP dataset from a CO_2 sequestration project in Western Canada. In this paper,

however, we primarily focus on testing a standard FWI algorithm using simulated VSP data in Matlab.

TIME DOMAIN FULL WAVEFORM INVERSION IN MATLAB

The FWI procedure that we followed to simulate VSP data herein is adapted from the Romahn (2019) workflow, with two major subdivisions: a synthetic environment to simulate a seismic acquisition experiment and the main FWI algorithm. Although, this adaptation shares a similar scheme and usage of Matlab functions from the CREWES toolbox, it also has significant differences, which are noticeable in two key FWI steps: the calculation of the gradient and the estimation of the step-length to calibrate an update.

Initial model and acquisition design

The initial velocity model is computed by a smoothing process of the true velocity model, which is done by convolving a Gaussian with the slowness model (inverse of the true velocity) and then inverting the result, in order to roughly preserve the traveltime. To create the Gaussian, the only input parameter needed would be its half-width.

Next, the model acquisition geometry is stablished by providing the number of receivers and sources, and allowing the program to automatically calculate their distribution, both locations and spacing, keeping equal distance between them, unless otherwise specified by the user. Several types of seismic experiments can be modeled while varying their geometry, from surface seismic to VSP. For this investigation both types of arrays were tested, but ultimately a VSP geometry was utilized to analyze further details.

At the time of this report, two profile locations can be chosen for a quick examination of the velocity update throughout the inversion and its comparison to the true velocity. In order to set these locations, the horizontal positions of the profiles must be introduced in meters.

The final output of this part of the program is a Matlab file with matrices for the true velocity and initial velocity models, vectors with horizontal and depth coordinates of the model, vectors with the horizontal and depth distribution of the sources and receivers, the indices of the chosen profiles and the values of maximum and minimum velocity of the true model at the profile locations.

Time domain full waveform inversion

The main FWI programme is subdivided in a set up section and an inversion algorithm that follows a classical FWI workflow, as illustrated in Figure 1, and that incorporates several Matlab functions available in the CREWES toolbox.

In the set up segment, the user can choose the minimum and maximum plot limits, set the dominant frequency of the wavelet and introduce parameters, like the size of time step for modeling (in seconds), the size of the time sample rate for the output seismogram (in seconds), the seismogram length (in seconds), the Laplacian approximation (5 or 9 point approximation) and the boundary conditions (0 for no absorbing, 1 for all sides absorbing and 2 for three absorbing sides), all which will be necessary for the finite difference approximation. In addition, the user can define the low-cut and high-cut of frequencies to

be migrated (in Hz) and number of iterations defined by the starting and ending points, which are suffixed to the names of the files saved after an iteration is completed.

The algorithm saves a Matlab file on the hard drive after each iteration containing a matrix of the current velocity model update and vectors with the data misfit (overall and normalized values). This format allows the user to stop and re-start the inversion process from an exact stage using a function that will load the updated matrix of the velocity model that precedes the chosen starting iteration, but only if it is different than one. Next, it will either compute or load the observed dataset and display two plots, one with velocity models, both true and the current update, and another with the two profiles and the normalized data misfit.

Once initialization is complete, the main algorithm will display a message with the estimated time for the inversion in the command window. The first step in a standard FWI workflow is solving the forward problem to generate a synthetic dataset by wave propagation modeling, which is properly done using an acoustic finite difference approximation from the CREWES toolbox. After this, the data residuals are computed using the L2 norm between observed and synthetic data, and an overall misfit per iteration is be stored and normalized for comparison purposes.

The following step in the algorithm is to compute an uncalibrated update known as the gradient, which requires calculating the partial derivatives of an objective function throughout all the points in the model. This calculation involves a significant computational burden, which is overcome by utilizing a reverse time migration (RTM) of the residuals, constructed using a crosscorrelation imaging condition, which is equivalent to the FWI gradient (Margrave et al., 2012). This migration of the residuals entails a multiscale approach applying a bandpass filter defined by the low and high-cut frequencies preset by the user, which ultimately makes its cost directly proportional to the number of frequencies migrated.

After the update direction leading towards the global minimum is calculated, the gradient itself needs to be calibrated at each spatial point to make it proportional to the velocity change (Vigh et al., 2009). This is achieved by a minimization of the objective function with respect to the step-length, as proposed by Tarantola (1984) and Pica et al., (1990). In the algorithm a scalar step-length is computed using two terms denoted as “Pica A” and “Pica B”, where the first describes how the modeled wavefield changes with respect to the step-length given an update direction and the second is the residual between observed and synthetic data at the current iteration. Once estimated, the multiplication of the update direction by the scalar step-length is made and a global update in the model space is done.

INVERSION RESULTS USING SIMULATED VSP DATA

A shallow anticline model with a low-velocity reservoir surrounded by relatively high-velocity intervals, as illustrated in Figure 2, was the earth model chosen to test the algorithm. An arrangement of 101 downhole receivers starting from the surface and equally spaced each 10 m within 1 km of depth was a consistent configuration throughout the inversion, as well as the location of the profiles, which were located at 690 m and 200 m

from the receivers. The distribution of equidistant sources varied between 21 and 41, depending the objectives of the inversion.

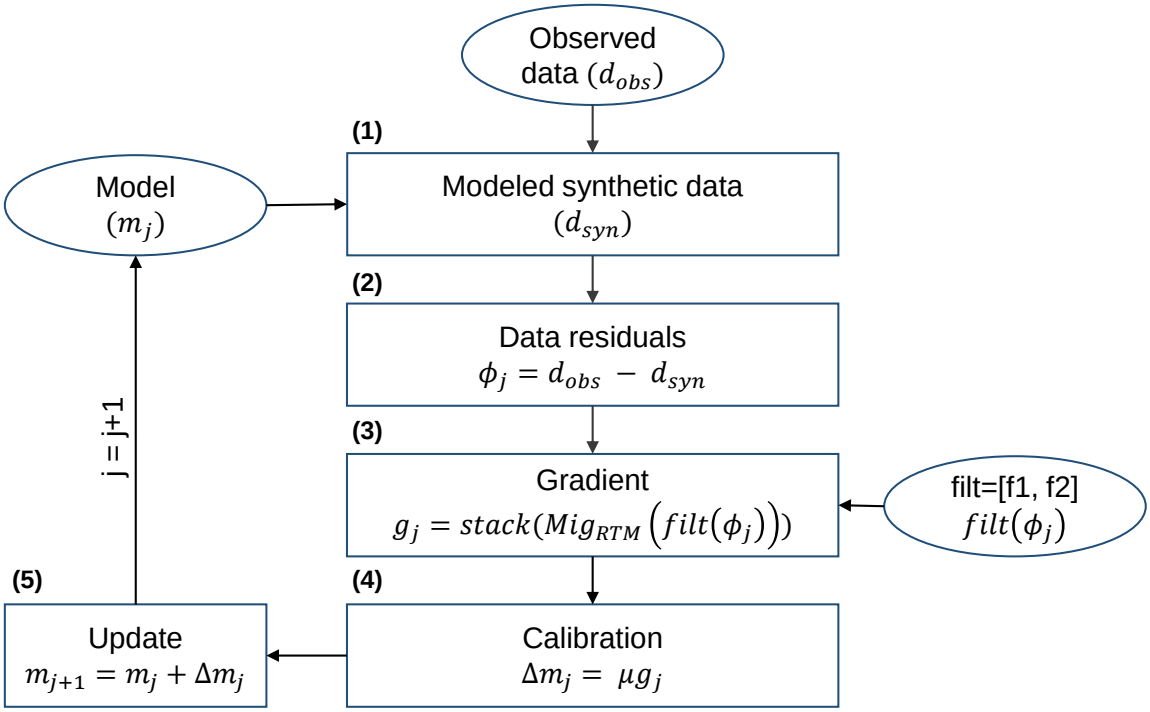

FIG. 1. FWI workflow utilized in this investigation. The iterative cycle is divided into five main steps: (1) modeling a synthetic dataset, (2) calculation of data residuals, (3) computation of the gradient as an update direction, (4) calibration of the update direction by a scalar step-length, and (5) updating the model. Adapted from Romahn (2019).

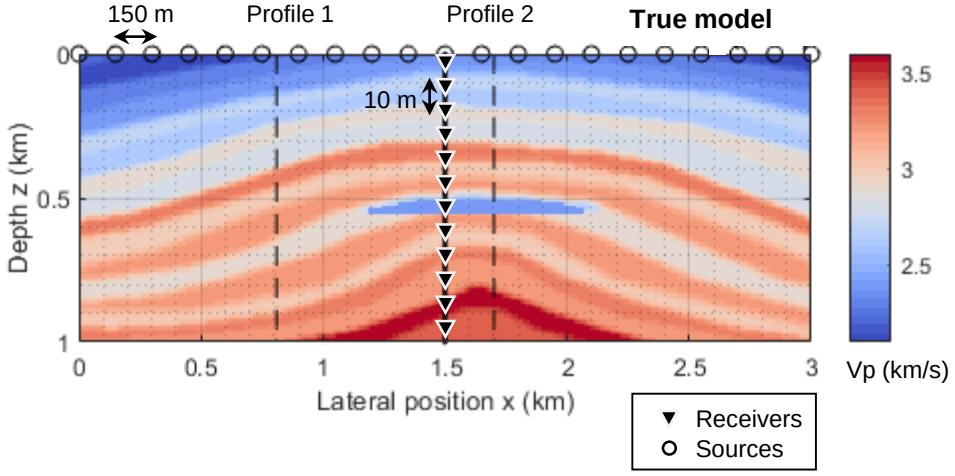

FIG. 2. True P-wave velocity model overlain by the acquisition design for the simulated VSP dataset. Borehole location is set at the lateral position of 1.5 km and receivers are equally spaced from surface to bottom depth every 10 m at the same location. An arrangement of sources is defined on the surface every 150 m. Black triangles and dots indicate receivers and sources, respectively.

Resolution of VSP data in model space

The acquisition geometry of VSP datasets results in seismograms that are typically dominated by transmitted wavefields rather than reflection events. This characteristic highlights one of the major differences in shot gathers, when compared with traditional surface seismic. This also implies an exponential decrease of illumination of subsurface features with increasing offsets. For large offsets the number of ray paths that will travel and be recorded in the receivers will be less abundant than for near offsets and this has immediate implications in FWI.

Figure 3 shows the inverted model after 96 iterations using a multiscale approach of expanding frequency bands between [1 Hz, 3 Hz] up to [31Hz, 33Hz], where the low-cut frequency was increased as well as the high-cut, after reaching 3 iterations per band. The top rows (a) and (b) display the initial and inverted P-wave velocity model, while (c) and (d) present the detailed updates of the velocity for the profile locations. Although, the inverted model reproduces significantly well the area close to the receivers using only low to medium frequencies, a decrease of lateral resolution in the model space is both noticeable and expected. As previously mentioned, the ray paths that cover large offset decrease and therefore, any capability of resolving features in those areas using FWI diminish.

Resolution in the model space using VSP does not only decrease laterally, but it also does vertically in a cone-shaped fashion. The bulk of transmitted and reflected events, which in a shot gather we will refer to as downgoing and upgoing waves respectively, illuminate shallow intervals with ample coverage. However, as depth increases, deep intervals are sparsely sampled leading into an upward cone-shaped illumination pattern from bottom to top in depth. The radius of the cone is mainly controlled by the distribution of sources and receivers in an acquisition survey, and it is a distinguishing feature of VSP datasets.

Trade-off of two multiscale schemes

We employed two multiscale schemes for the expansion of frequency bands, and results suggest an interesting trade-off between model and data space. For one of the approaches, the low-cut limit was kept constant and only the upper cut was expanded while in the other case both low and high-cut limits continued to expand after reaching convergence in a specific band. In both cases, the low-cut and high-cut limits were set at 5 Hz and 40 Hz, respectively.

In Figure 4, (a) and (b) represent the inverted models from a low band [5Hz, 20 Hz] and a medium band [5Hz, 40Hz] frequency with a fixed low-cut limit. These results display convergence in model space at low frequencies and no further improvement when utilizing medium frequencies. Meanwhile, in Figure 4, (c) and (d) are the inverted models from a low band [15Hz, 20 Hz] and a medium band [35Hz, 40Hz] frequency with a moving window in the frequency domain. They illustrate a comparable result with the first scheme for low frequencies, but altogether an inferior resolution in model space for medium frequencies, even for depth intervals that were well resolved in previous bands.

Convergence behaviour observed in model space is also traceable in the data space. Figure 5 displays the normalized data misfit per iterations, and though there is a predominant downhill trend at the beginning of each frequency band, it is then followed by convergence. For the inverted models using a constant low-cut in frequency, data misfit converges within the first 100 iteration, which is associated with the low frequency spectrum and, just as model space shows, there is no further change for medium frequencies. On the other hand, a moving window in frequency domain maintains a downward trend in the residuals, which is always desirable in FWI; but as shown in Figure 4(d), this does not guarantee that resolution in model space is improved.

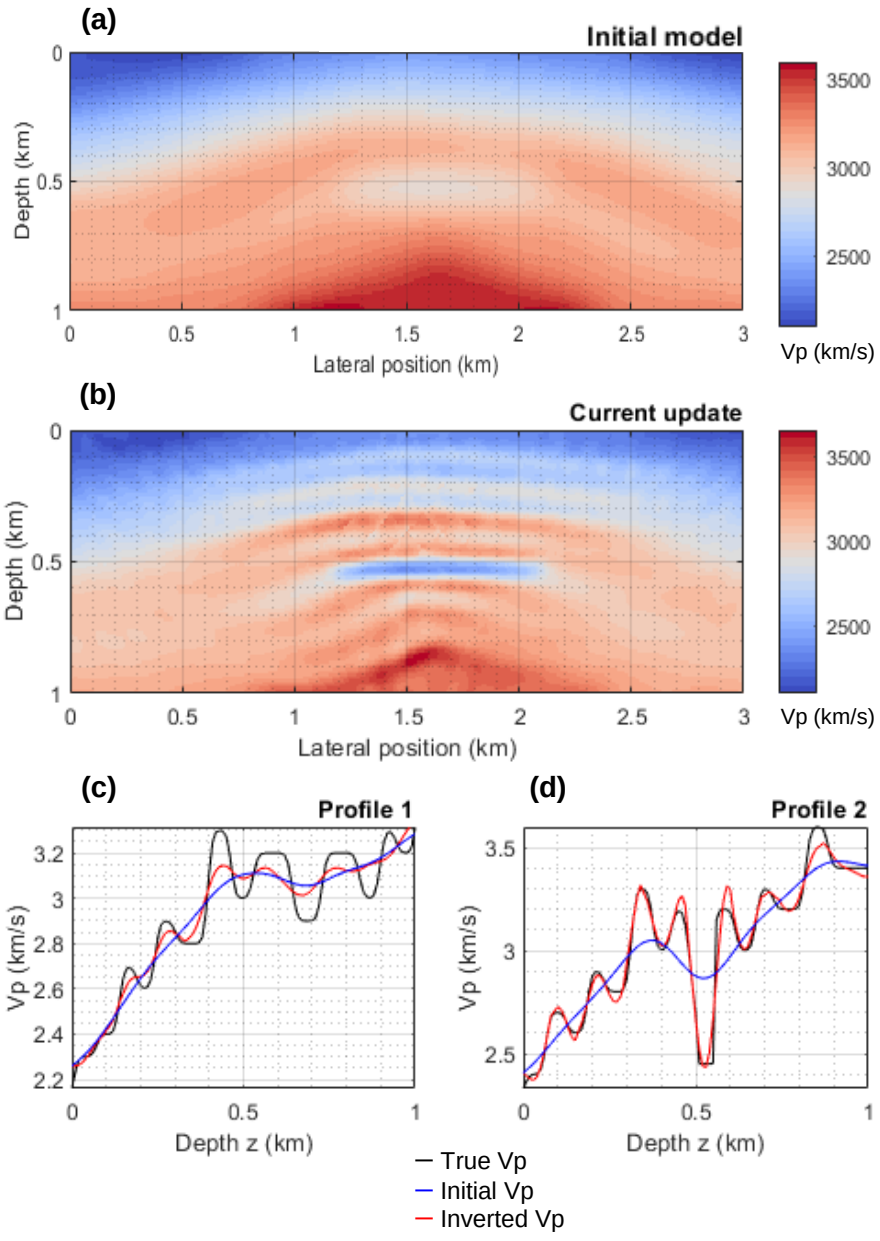

FIG. 3. P-wave velocity at (a) initial model, (b) inverted model, (c) profile location 1 distanced 690 m from centered receivers and (d) profile location 2 distanced 200 m from centered receivers after 96 iterations, using a moving frequency window approach between 1 Hz to 33 Hz.

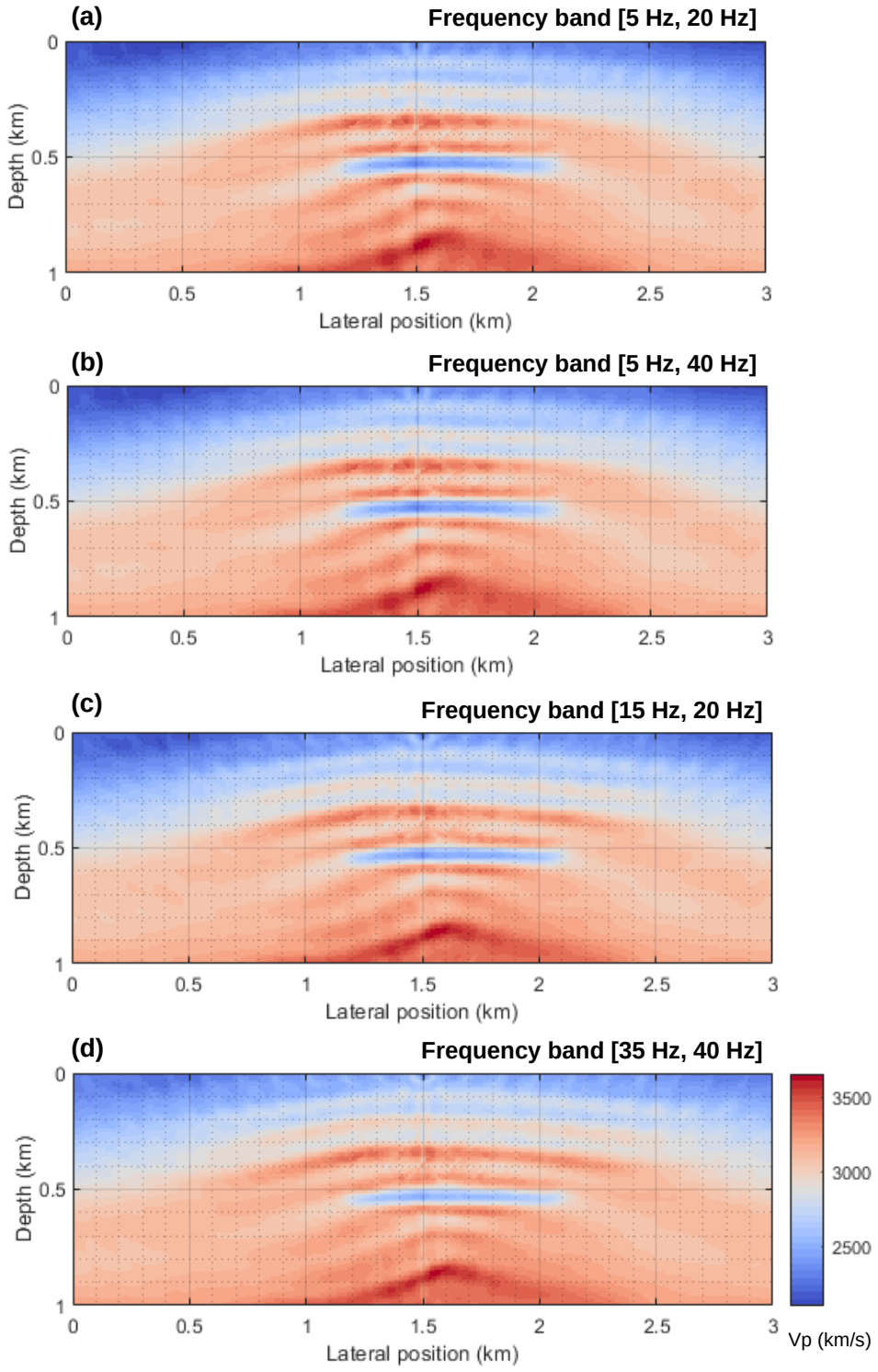

FIG. 4. Inversion results using two different multiscale schemes. Inverted models using a constant low-cut limit in the frequency at a (a) low band and (b) medium band frequency. Inverted models using a moving low and high-cut limit in the frequency at a (c) low band and (d) medium band frequency.

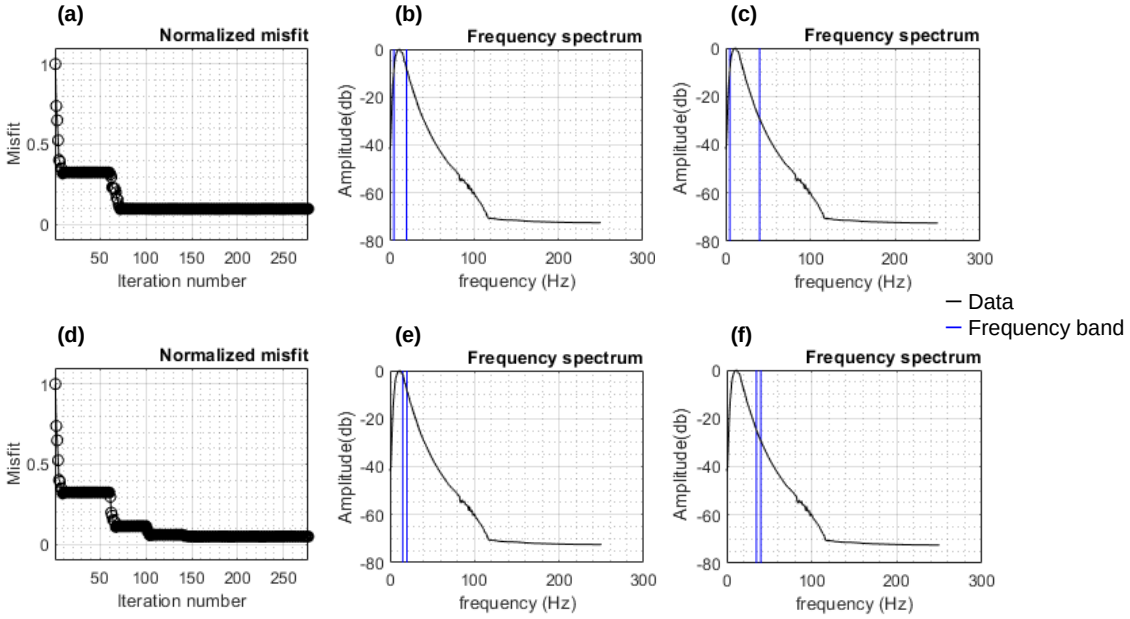

FIG. 5. Follow up of two multiscale schemes in the data misfit and in the frequency spectrum. Inversion using a constant low-cut limit in frequency: (a) normalized data misfit plot per iteration, (b) frequency spectrum for a low frequency band between [5 Hz, 20 Hz], and (c) frequency spectrum for a medium frequency band between [5 Hz, 40 Hz]. Inversion using a moving low and high-cut limit in the frequency: (d) normalized data misfit plot per iteration, (e) frequency spectrum for a low frequency band between [15 Hz, 20 Hz], and (f) frequency spectrum for a medium frequency band between [35 Hz, 40 Hz].

A plausible explanation for the stated behaviour is associated with the frequency spectrum of the data, which is intrinsically related to the source signal used. Our simulated dataset was modeled with a 10 Hz minimum phase wavelet and as Figure 5 illustrates, low frequencies contained most of the information needed to resolve the features of our model. Consequently, once the frequency band that contains key and resolvable features of the model by the employed wavelet is fully utilized, there will not be information left to add in the data space and hence, not much enhancement in the model space. Nonetheless, even when the same wavelet and general parameters were employed in the second multiscale approach, there is a slight decrease in data misfit and changes in the model space at the beginning of medium frequencies, which is probably associated with the band usage at each stage of the inversion. While low frequencies resolve general trends of a model, medium to high frequencies add fine details; consequently, using a moving window will tend to emphasize resolution of some details over others.

Source footprint

Artifacts in inversion are undesirable noises that either have a profound impact that could mislead the results, or simply introduce unappealing marks in the model space. Although, this algorithm has proven to invert for promising models using synthetic datasets, it does not escape from the unwanted effect of source footprint in some inverted models. Figure 6 shows inversion results from the frequency bands [12 Hz, 14 Hz] and [23 Hz, 25 Hz] for the same receiver disposition, but employing 21 and 41 sources equally

spaced within 3 km. It is noticeable that increasing the number of sources does not entirely reduce a source footprint from the inversion, but at least it decreases its effect.

A distribution of 31 sources was also tested; however, it did not diminish the source footprint. Hence, to reproduce optimum earth models images using VSP, it is encouraged to test several acquisition designs, with special emphasis on the number of sources to utilize. A small number of iterations (around 10) will provide a rough idea of the presence of this type of artifact.

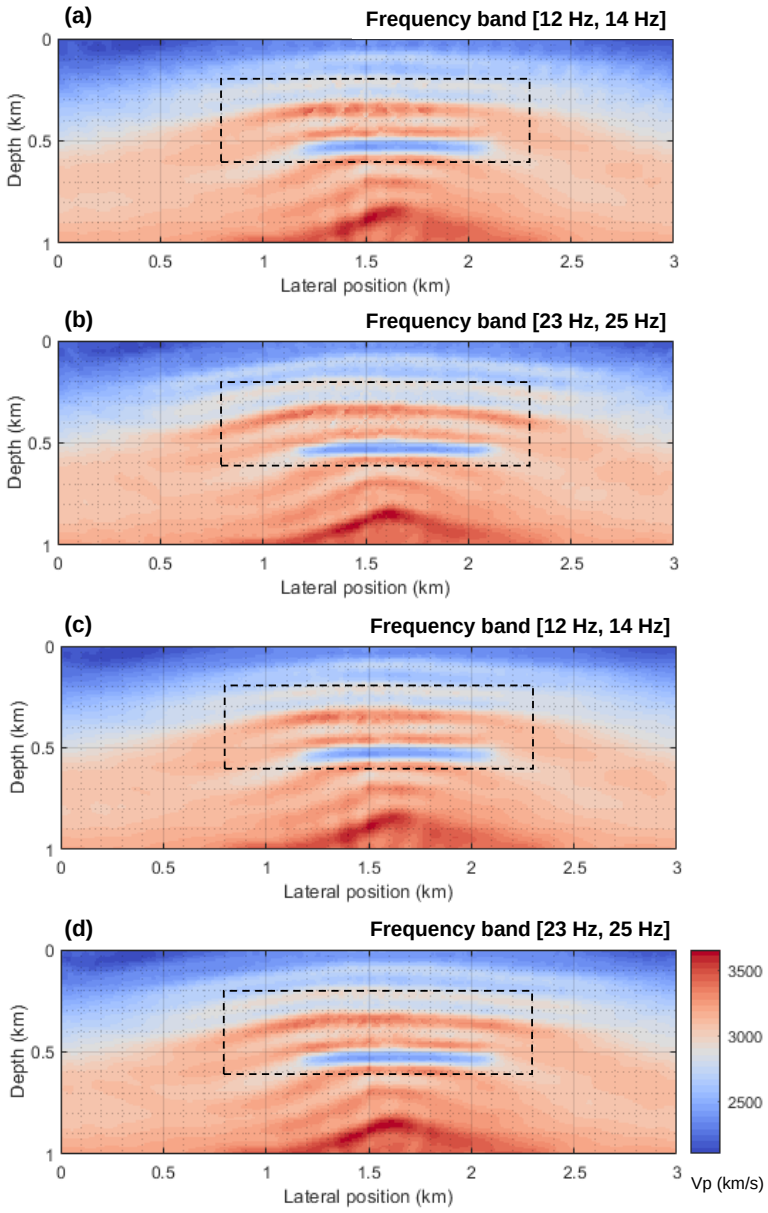

FIG. 6. Source footprint for two different source arrangements using a moving frequency window approach between 1 Hz to 25 Hz. Inverted model utilizing 21 sources equally spaced every 150 m at a frequency band (a) [12 Hz, 14 Hz] after 36 iterations and (b) [23 Hz, 25 Hz] after 75 iterations. Inverted model utilizing 41 sources equally spaced every 75 m at a frequency band (c) [12 Hz, 14 Hz] after 36 iterations and (d) [23 Hz, 25 Hz] after 75 iterations.

CONCLUSIONS

Inversion of a simulated VSP dataset in Matlab was conducted using an acoustic FWI algorithm in time domain. Results in model space reproduce high-resolution images for a shallow low-velocity reservoir zone located in an antiform, which encourages us to infer that less complex structures will be also resolvable using this algorithm. However, due to the acquisition geometry of VSP, the influence of transmitted waves instead of reflected waves, and a sparse ray path coverage at large offsets associated with the experiment itself, resolution of inverted models considerably decreases both laterally and vertically with increasing offsets, exhibiting an inverted cone profile with depth.

Though, the algorithm is based in a multiscale approach, allowing a user to set the low and high-cut limit in frequency that is used during the gradient calculation as a bandpass filter for the migration of data residuals, updates in data and model space are predominantly controlled by the characteristic of the wavelet and to some degree, on the multiscale scheme chosen. Two procedures were explored using the same VSP acquisition geometry, one with constant low-cut frequency and another with a moving frequency window, both reaching the same high-cut frequency. Results vary in speed of convergence, the value of final data misfit, and resolution in the model space, which in both cases displayed the characteristic cone-shape associated with VSP surveys but differ in the level of detail that each prioritized.

ACKNOWLEDGEMENTS

The authors thank the sponsors of CREWES for continued support. This work was funded by CREWES industrial sponsors, and NSERC (Natural Science and Engineering Research Council of Canada) through the grants CRDPJ 461179-13 and CRDPJ 543578-19. The acoustic FWI code utilized in this investigation was adapted from S. Romahn thesis, for which he is gratefully acknowledged. For editing and valuable suggestions, thanks to David Henley and Raul Cova.

REFERENCES

Cova, R., Innanen, K. A. H., and Rauch-Davies, M., 2018, Walkway VSP data conditioning for FWI: CREWES Research Report, **30**, 08.

Egorov, A., Pevzner, R., Bóna, A., Glubokovskikh, S., Puzyrev, V., Tertyshnikov, K., and Gurevich, B., 2017, Time-lapse full waveform inversion of vertical seismic profile data: Workflow and application to the CO2CRC Otway project: Geophysical Research Letters, **44**, 7211–7218.

Margrave, G. F., K. A. Innanen, and M. Yedlin, 2012, A Perspective on Full-Waveform Inversion: CREWES Research Report, **24**, 70.

Pan, W., Innanen, K. A., and Geng, Y., 2018, Elastic full-waveform inversion and parametrization analysis applied to walk-away vertical seismic profile data for unconventional (heavy oil) reservoir characterization: Geophysical Journal International, **213**, 1934–1968.

Pica, A., J. Diet, and A. Tarantola, 1990, Nonlinear inversion of seismic reflection data in a laterally invariant medium: Geophysics, **55**, 284–292.

Podgornova, O., Leaney, S., Charara, M., and Lunen, E. V., 2014, Elastic full waveform inversion for land walkaway VSP data: CSEG Geoconvention 2014 Expanded abstracts.

Romahn, S., 2019, Well-log validated waveform inversion of reflection seismic data: Doctoral dissertation, University of Calgary.

Tarantola, A., 1984, Inversion of seismic reflection data in the acoustic approximation: Geophysics, **49**, 1259–1266.

Vigh, D., E. W. Starr, and J. Kapoor, 2009, Developing earth models with full waveform inversion: The Leading Edge, **28**, 432–35.